

Simulation of Turbulence Pressure Fluctuations on Cylinders In Axial Flow

M.J. Woods and M.K. Bull
 Department of Mechanical Engineering
 The University of Adelaide, SA, 5005, AUSTRALIA

Abstract

Direct numerical simulations have been made of the turbulent boundary layer developed in axial flow over long cylinders. In the frequency spectra of surface-pressure fluctuations on the cylinders, characteristic frequency ranges, which are the counterparts of similar ranges in flat-plate flow, have been identified. Forms of similarity scaling in these ranges have been determined. They are considerably more complicated than the flat-plate scaling, with length and time scales additionally dependent on curvature parameters, but are consistent with existing numerical simulations of and experimental data for cylinder flows.

At the low cylinder Reynolds numbers considered, the rms surface-pressure in terms of the mean wall shear stress is found to be smaller than in flat-plate flow; it increases towards flat-plate values as the cylinder Reynolds number increases, in accord with experiment.

Introduction

Properties of the axisymmetric turbulent boundary layer that develops on a very long cylinder with its axis aligned with the direction of a uniform flow of fluid have been determined by direct numerical simulation. Details of the numerical method are given by Woods and Bull [8]. The procedure is similar to that used by Neves, Moin and Moser [5], with the exception that the boundary conditions at the cylinder surface and at the outer edge of the boundary layer have been set in terms of vorticity rather than velocity.

Here, attention is concentrated on the pressure fluctuations generated at the cylinder surface. The cylinder radius is denoted by a , the fluid kinematic viscosity by ν , the free-stream velocity by U_1 , and the boundary layer thickness by δ . Flows with cylinder Reynolds numbers of $Re_a = U_1 a / \nu = 311, 492, 674$ and 1300 and various values of the ratio δ/a have been considered. Two of the Reynolds number values, 311 and 674 are the same as those used in [5]. At $Re_a = 311$, calculations have been made for a systematic variation of δ/a over the range $4.0 \leq \delta/a \leq 28.3$. So far in the present work, direct calculations of frequency spectra and convection velocities have not been made. The frequency spectra presented have been obtained from calculated wavenumber spectra by application of Taylor's hypothesis, whereby the wavenumber k is replaced by ω/U_c , the radian frequency ω divided by the convection velocity U_c . The convection velocity has been taken as the value obtained by Neves et al. [5], namely $U_c = 0.65U_1$. The flow conditions considered are shown in Table 1.

Of direct interest is the effect of curvature on the frequency spectrum and the mean square pressure, as compared with the much more extensively investigated case of flow over a flat plate.

$Re_a/$ Ref.	δ/a	δ^+	Symbol	$Re_a/$ Ref.	δ/a	δ^+	Symbol
311	3.95	88.3	[5]	5	214	— ■ ·
311	7.25	160	-----	[5]	11	239	— —
311	14.8	310	-----	[3]	0	1169
311	28.3	573	———	[3]	0	2010	· - - ·
492	7.85	247	[6]	0	556	○
674	3.66	157	- · - ·	[1]	3.2	563	- - -
674	8.09	330	- - -	[1]	6.6	1101
1300	3.63	270	———	[1]	11.5	1829	— · ·
[4]	0	590	■ ■ ■ ■	[7]	5.04	892	— —

Table 1. Flow parameters and symbols used for figures.

Analysis of experimental investigations of surface-pressure fluctuations generated by the turbulent boundary layer on a flat plate (for example, Farabee and Casarella [3], Bull [2]) have shown that the power spectral density of the pressure ϕ scales in different ways in different frequency ranges. The following four frequency ranges and their associated forms of spectral scaling can be identified:

1. Low-frequency range: $\omega\delta^*/U_1 \leq 0.03$,
 $\phi U_1 / q^2 \delta^* = k_1 (\omega\delta^*/U_1)^2$;
2. Mid-frequency range: $5 \leq \omega\delta/U_\tau \leq 100$,
 $\phi U_\tau / \tau_w^2 \delta = f_2 (\omega\delta/U_\tau)$;
3. Universal range: $100 \leq \omega\delta/U_\tau \leq 0.3\delta^+$,
 $\omega\phi / \tau_w^2 = k_3$;
4. High-frequency range: $\omega^+ = \omega\nu/U_\tau^2 \geq 0.3$,
 $\phi^+ = \phi U_\tau^2 / \tau_w^2 \nu = f_4 (\omega\nu/U_\tau^2)$;

where δ^* is the displacement thickness of the boundary layer, τ_w the wall shear stress, $U_\tau = \sqrt{\tau_w / \rho}$, ρ is the fluid density, $q = (1/2)\rho U_1^2$, $\delta^+ = \delta U_\tau / \nu$, k_1 and k_3 are constants, and f_2 and f_4 represent functions. These scalings and frequency ranges make an obvious point of reference for the examination of similar results for axisymmetric boundary layers.

Low-frequency Range

The present cylinder calculations are based on periodic boundary conditions in the streamwise direction, with a periodic streamwise length in all cases of $66\pi a$. This limits the lowest attainable wavenumber to $k = 1/33a$ and the lowest attainable value of both $k\delta$ and $\omega\delta/U_c$ to $(\delta/a)/33$. The minimum possible value of $\omega\delta^*/U_1$ (for $\delta/a \approx 4$, $\delta/\delta^* \approx 6$, $U_c/U_1 = 0.65$) is therefore about 0.013. For larger values of δ/a , the parameter $\omega\delta^*/U_1$ exceeds the upper limit (0.03) of the flat-plate low-frequency range. Consequently comparison of axisymmetric-flow similarity and flat-plate similarity in this frequency range cannot usefully be made.

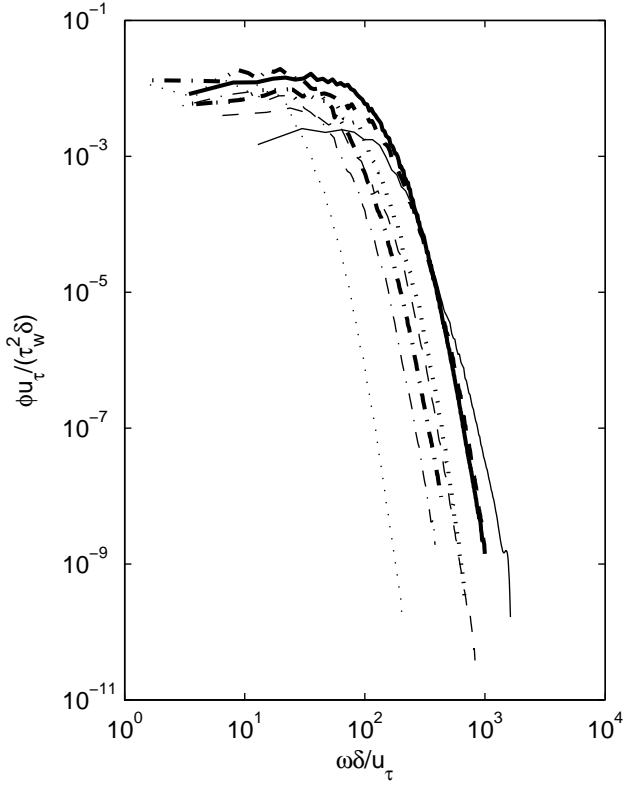


Figure 1. Pressure spectra of present simulations in flat-plate mid-frequency-range form. Symbols are defined in table 1.

Medium-frequency Range

When plotted in the flat-plate medium-frequency-range (MFR) form, $\phi U_\tau / \tau_w^2 \delta$ as a function of $\omega \delta / U_\tau$ (figure 1), the calculated data do not exhibit similarity.

Since it is to be expected that the greatest contributions to the wall pressure come from the regions closest to the wall, contributions from the outer part of the boundary layer can be expected to become less and less significant as δ/a increases. This suggests that the boundary layer thickness itself is unlikely to be the most appropriate length scale for this frequency range. In fact, the data collapse quite well when the radius of curvature, the cylinder radius, is used as the length scale instead of the boundary layer thickness. However, in the limiting case of very small δ/a , when the cylinder becomes effectively a flat plate with $a = \infty$, the radius of curvature ceases to be a useful length scale and must be replaced by the boundary-layer thickness. A possible composite length scale L that meets the limiting requirements at the extremes of very large and very small δ/a can be defined as

$$L = \delta / [1 + (\delta/na)] = Fa, \quad (1)$$

where

$$F = (\delta/a) / [1 + (\delta/na)], \quad (2)$$

and n is a constant factor, an appropriate value of which is a low integer. A similar factor has been used by Neves et al. [5], although in their case to increase the length scale to a value larger than δ rather than to decrease it as in the present case. Equation (1) has the property that $L \rightarrow na$ as $\delta/a \rightarrow \infty$ and $L \rightarrow \delta$ as $\delta/a \rightarrow$

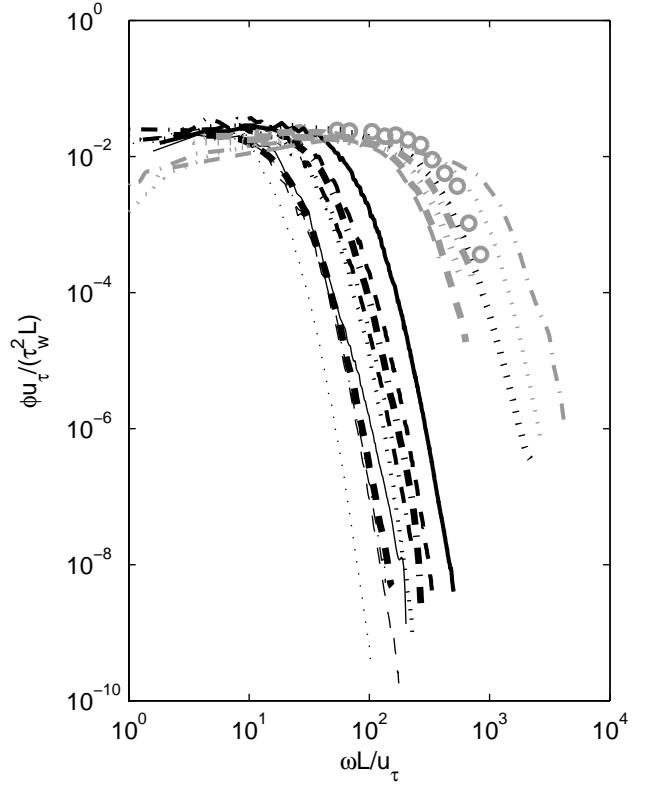


Figure 2. Pressure spectra in modified mid-frequency form, with $L = \delta / [1 + \delta/4a]$ (see equation 1). Symbols are defined in table 1.

0. Similarity of the results of the present calculations is not very sensitive to the value of n : it is quite close for values of n from about 1 to 4. A value of $n = 4$ has been chosen as this seems to give the most satisfactory agreement with flat-plate data. For δ/a as low as 4, $L = 2a = \delta/2$, L is still heavily biased towards the cylinder radius.

The data in the modified form $\phi U_\tau / \tau_w^2 L = \phi U_\tau (1 + \delta/4a) / \tau_w^2 \delta$ as a function of $\omega L / U_\tau = \omega \delta / (1 + \delta/4a) U_\tau$ are shown in figure 2. In this form there is similarity, with $\phi U_\tau / \tau_w^2 L$ constant over the lower part of the frequency range. The calculations indicate that the constancy persists at least down to a frequency corresponding to $\omega L / U_\tau \approx 0.2$, while the upper limit is Reynolds-number dependent and given approximately by $\omega L / U_\tau = 0.2L^+$ (where $L^+ = LU_\tau/\nu$). The range can therefore be tentatively taken as $0.2 \leq \omega L / U_\tau \leq 0.2L^+$. This contrasts with the approximate constancy of $\phi U_\tau / \tau_w^2 \delta$ over the flat-plate mid-frequency range of $5 \leq \omega \delta / U_\tau \leq 100$. Other cylinder data — the results of the numerical simulations of Neves et al. [5] and the experimental results of Snarski and Lueptow [7] and Berera [1] — are consistent with this, as figure 2 indicates. The Reynolds-number dependency of the upper limit of this frequency range is a reflection of the fact that at these low Reynolds numbers the overall rms pressure fluctuation is strongly dependent on the cylinder Reynolds number.

High-frequency Range

At a given value of the cylinder Reynolds number (Re_a), spectral plots (figure 3) in the flat-plate high-frequency (HFR) form, $\phi^+ = \phi U_\tau^2 / \tau_w^2 \nu$ as a function of $\omega^+ = \omega \nu / U_\tau^2$, show close similarity that is almost independent of the value of δ/a . For all the Reynolds numbers considered, the similarity occurs for ω^+ greater than

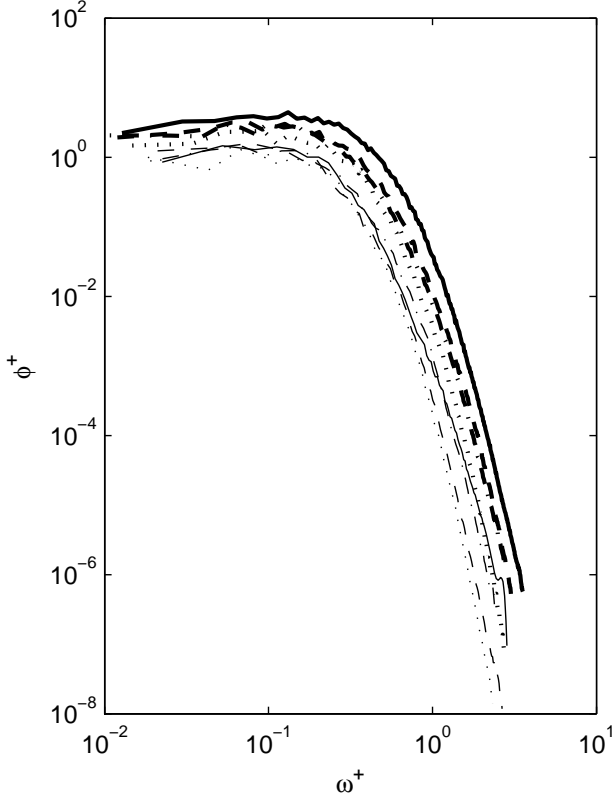


Figure 3. Pressure spectra of present simulations in flat-plate high-frequency-range form. Symbols are defined in table 1.

0.2–0.3, a value very similar to that for high-frequency similarity in the flat-plate case. However, the similarity curve is not the same at all Reynolds numbers, the spectral levels increasing with Re_a (or $a^+ = aU_\tau/\nu$ or L^+), a further reflection of the fact that at these low Reynolds numbers p'/τ_w is quite strongly dependent on Re_a . Nevertheless, the curves do have similar forms, and those for the various Reynolds numbers can be brought together if the data are plotted in the form of $G^2\phi^+$ against $G\omega^+$ (figure 4), where G is primarily a function of a^+ (although also expressible in terms of F and L^+); G can be represented empirically as

$$\begin{aligned} G &= (1 + 120/a^+)^{1/2} \\ &= (1 + 120F/L^+)^{1/2}. \end{aligned} \quad (3)$$

As a^+ and L^+ increase, the function G approaches unity, so that for large values of these parameters the standard flat-plate spectral form of ϕ^+ as a function of ω^+ is recovered.

Universal Frequency Range

The flat-plate universal range represents an overlap of the mid-frequency and high-frequency ranges. Such an overlap implies that, in this range, the spectral density is independent of any frequency scale, which in turn implies that $\phi \propto \omega^{-1}$ or $\omega\phi = \text{constant}$. For the present cylinder data, the character of the variation of the spectral density with increasing frequency — a transition from a constant value to a rapidly falling value — inevitably means that over some part of the frequency range the spectral density will vary inversely as the frequency. The frequency range over which this form of variation occurs is in fact very small, and there is certainly no extended region of overlap as found in high-Reynolds-number measurements on flat

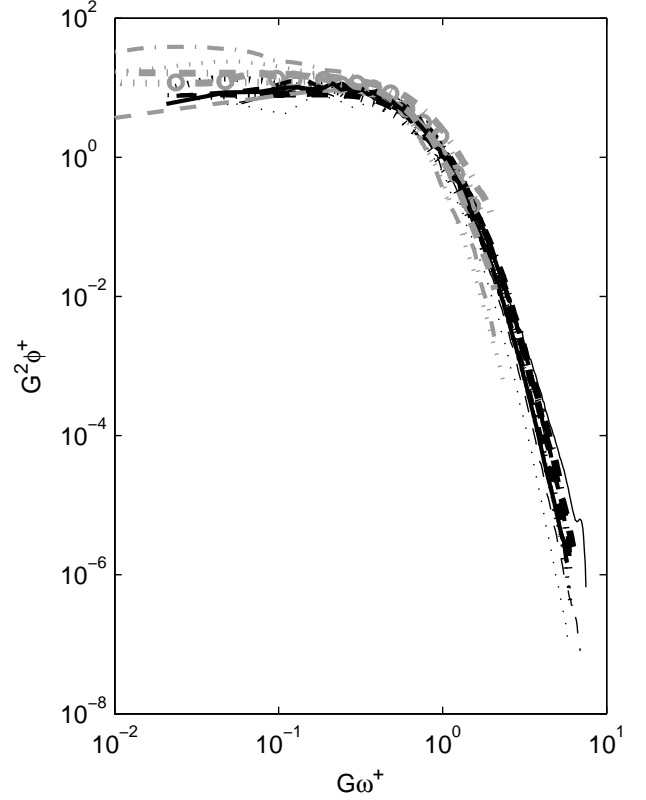


Figure 4. Pressure spectra in modified high-frequency form, with G given by equation 3. Symbols are defined in table 1.

plates. For the low Reynolds numbers under consideration, the upper limit of the mid-frequency range and the lower limit of the high-frequency range can therefore be taken to be coincident. The high-frequency range can then be defined by $G\omega^+ \geq 0.2G$, that is $\omega^+ \geq 0.2$.

Mean-square Pressure

Calculated and experimental values of the rms wall-pressure fluctuation p' , expressed in the form of p'/τ_w (where τ_w is the mean shear stress at the cylinder surface), are shown in figure 5 as a function of L^+ . An empirical expression for p'/τ_w can be obtained from the values of the non-dimensional spectral levels in the frequency ranges that have been identified and the corresponding non-dimensional extents of those ranges. Thus, the contribution of the "mid"-frequency range (where $\phi U_\tau/\tau_w^2 L = \text{constant} = 0.020$) to the mean square pressure is

$$\overline{(p'^2/\tau_w^2)}_{\text{MFR}} = (0.020) (0.2L^+) = 0.0040L^+. \quad (4)$$

(This assumes that the constant value of $\phi U_\tau/\tau_w^2 L$ also extends over the frequency range $0 \leq \omega L/U_\tau \leq 0.2$, but the contribution from this range will generally be insignificant).

With the extent of any overlap region assumed to be negligible, the contribution of the high-frequency range to the mean square pressure is

$$\overline{(p'^2/\tau_w^2)}_{\text{HFR}} = (1/G^3) \int_{0.2G}^{\infty} (G^2\phi^+) d(G\omega^+). \quad (5)$$

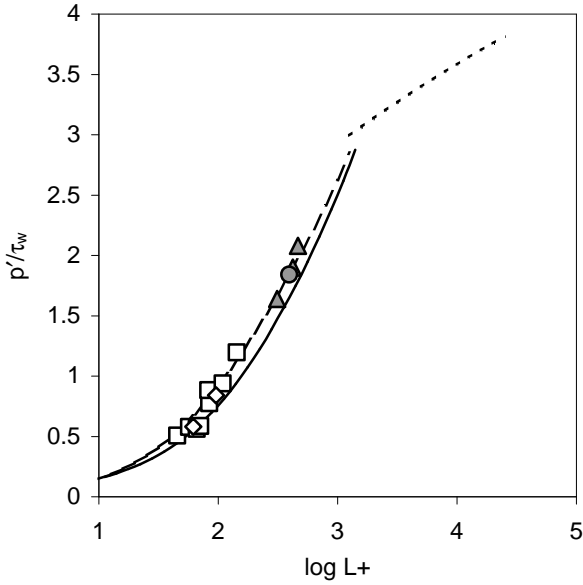


Figure 5. Root-mean-square pressure normalised by mean wall shear stress as a function of length scale L^+ . Equation (7): --- $\delta/a=4$; — $\delta/a=30$. Equation (8): - - - ($L^+=\delta^+$). Simulations: \square present study; \diamond [5]. Experiments: \triangle [1]; \bullet [7].

Evaluation of the integral leads to the result

$$\overline{(p^2/\tau_w^2)}_{\text{HFR}} = 5.75/G^3 - 1.60/G^2. \quad (6)$$

The total mean square pressure is then given by

$$\begin{aligned} p'/\tau_w &= [(\overline{p^2/\tau_w^2})_{\text{MFR}} + (\overline{p^2/\tau_w^2})_{\text{HFR}}]^{1/2} \\ &= [0.0040L^+ + 5.75/G^3 - 1.60/G^2]^{1/2}. \end{aligned} \quad (7)$$

This relation is compared with the available low-Reynolds-number experimental and numerical data for cylinders in figure 5. Its form implies a weak dependence on δ/a , as the curves for $\delta/a = 4$ and 30 (the approximate range of this parameter for the data considered) shown in the figure illustrate. In the limiting case of the flat plate, the scale L becomes the boundary layer thickness, and $L^+ = \delta^+$. The figure therefore also shows the form of the dependence on δ^+ of the rms pressure for flat plates at high Reynolds numbers as determined by Farabee and Casarella [3], namely

$$p'/\tau_w = [6.5 + 1.86 \ln(\delta^+/333)]^{1/2}. \quad (8)$$

Conclusions

Direct numerical simulations of the pressure fluctuations on the surface of a cylinder in axial flow show that the pressure spectra exhibit characteristic frequency ranges that are the counterparts of the frequency ranges previously identified for flow over flat plates. The cylinder ranges, however, show considerably more complicated similarity scaling relations than the flat-plate ranges,

as a result of the effects of curvature on the flow. These effects introduce a dependence on δ/a and a^+ in addition to the parameters governing flat-plate flow. Empirical forms for the spectral scaling have been obtained from the numerical simulations. These are consistent with available experimental data for cylinders in axial flow, and asymptotically approach the flat-plate relations as the radius of the cylinder increases. In particular, it is found that, for the low Reynolds numbers considered, the counterparts of the mid-frequency and high-frequency flat-plate ranges are:

$$\begin{aligned} \text{Mid-frequency range: } 0.2 \leq \omega L/U_\tau \leq 0.2L^+, \\ \phi U_\tau/\tau_w^2 L = f_2(\omega L/U_\tau); \end{aligned}$$

$$\begin{aligned} \text{High-frequency range: } \omega^+ \geq 0.2, \\ G^2 \phi^+ = f_4(G\omega^+). \end{aligned}$$

There appears to be no significant universal range in a region of overlap of the mid-frequency and high-frequency ranges.

At low cylinder Reynolds numbers Re_a , the ratio of mean-square surface-pressure to wall shear stress p'/τ_w is found to be considerably smaller than the values typical of flat plates, but to increase towards flat-plate values with increasing Re_a , a^+ , and the scale L^+ .

Acknowledgments

The support of this work by the Australian Research Council and Thales Underwater Systems is gratefully acknowledged.

References

- [1] Berera, F., *An Investigation of the Flow along and Induced Vibration of Long Cylinders*, Ph.D. thesis, Department of Mechanical Engineering, University of Adelaide, Australia, 2004.
- [2] Bull, M.K., Wall-pressure fluctuations beneath turbulent boundary layers; some reflections on forty years of research, *J. Sound Vib.*, **190**, 1996, 299–315.
- [3] Farabee, T.M. and Casarella, M.J., Spectral features of wall pressure fluctuations beneath turbulent boundary layers, *Phys. Fluids A*, **3**, 1991, 2410–2420.
- [4] Moser, R.D., Kim, J. and Mansour, N.N., Direct numerical simulation of turbulent channel flow up to $Re_\theta=590$, *Phys. Fluids*, **11**, 1999, 943–945.
- [5] Neves, J.C., Moin, P. and Moser, R.D., Effects of convex transverse curvature on wall-bounded turbulence, *J. Fluid Mech.*, **272**, 1994, 349–406.
- [6] Schewe, G., On the structure and resolution of wall-pressure fluctuations associated with turbulent boundary layer flow, *J. Fluid Mech.*, **134**, 1983, 311–328.
- [7] Snarski, S.R. and Lueptow, R.M., Wall pressure and coherent structures in a turbulent boundary layer on a cylinder in axial flow, *J. Fluid Mech.*, **286**, 1995, 137–171.
- [8] Woods, M.J. and Bull, M.K., Computation of the turbulent boundary layer on a long circular cylinder in axial flow with a vorticity boundary condition, in proceedings of ICCFD3, Springer, 2004.